Polymer Chemistry

# Thermal Annealing Effects on the Mechanical Properties of Bio-based 3D Printed Thermosets



| | |
|---|---|
| Journal: | *Polymer Chemistry* |
| Manuscript ID | PY-ART-02-2023-000200.R1 |
| Article Type: | Paper |
| Date Submitted by the Author: | 20-Apr-2023 |
| Complete List of Authors: | Cortés-Guzmán, Karen; University of Texas at Dallas, Chemistry and Biochemistry<br>Parikh, Ankit; The University of Texas at Dallas, Mechanical Engineering<br>Sparacin, Marissa; University of Texas at Dallas, Chemistry and Biochemistry<br>Johnson, Rebecca; University of Texas at Dallas, Chemistry and Biochemistry<br>Adegoke, Lauren; University of North Texas, Biomedical Engineering<br>Ecker, Melanie; University of North Texas, Biomedical Engineering<br>Voit, Walter; Department of Materials Science and Engineering, University of Texas at Dallas<br>Smaldone, Ronald; University of Texas at Dallas, Chemistry and Biochemistry |
| | |

# Thermal Annealing Effects on the Mechanical Properties of Bio-based 3D Printed Thermosets

Karen P. Cortés-Guzmán,[1] Ankit R. Parikh,[2] Marissa L. Sparacin,[1] Rebecca M. Johnson,[1] Lauren Adegoke,[4] Melanie Ecker,[4] Walter E. Voit,[2,3] Ronald A. Smaldone*[1,3]

[1]Department of Chemistry and Biochemistry, University of Texas at Dallas, 800 West Campbell Road, Richardson, Texas 75080, United States

[2]Department of Mechanical Engineering UT Dallas University of Texas at Dallas, 800 West Campbell Road, Richardson, Texas 75080, United States

[3]Department of Materials Science and Engineering UT Dallas University of Texas at Dallas, 800 West Campbell Road, Richardson, Texas 75080, United States

[4]Department of Biomedical Engineering, University of North Texas, 1155 Union Circle #310440, Denton, Texas 75203, United States

## Abstract

3D printing technologies can address many sustainability aspects of creating new materials, such as reduced waste and on demand production, which reduces the carbon footprint of transport and storage. Additionally, creating bio-based resins for 3D printing is a viable way of improving the sustainability of polymeric materials. Coupled with this, by using dynamic covalent chemistry (DCC), we can provide materials with smart properties like self-healing or reprocessability to either extend their usable lifetime or provide an alternative to the materials ending up in a landfill. Here, we report a series of completely bio-based aromatic resins for digital light projection (DLP) printing. By incorporating β-hydroxyesters and a zinc catalyst, the polymer networks can participate in transesterification reactions to provide self-healing capabilities or reprocessability. The self-healing abilities of these materials were characterized using optical microscopy, and the reprocessability using a hot-press. Additionally, by subjecting the printed thermosets to thermal annealing, considerable changes in the mechanical performance were observed leading to more than a 2000% increase in the Young's modulus. The thermal behavior after annealing was also studied and a discussion on the effect of the structural differences between the aromatic monomers is proposed. These resin formulations address two of the key goals of sustainable materials: using renewable resources and obtaining recyclable materials while remaining competitive through their mechanical performance and compatibility with 3D printing technologies.

**Keywords:** Vanillin, vitrimer, bio-based, 3D printing, dynamic covalent chemistry, covalent adaptable networks, transesterification, self-healing, thermally reprocessable.

## Introduction

Contemporary society relies heavily on polymeric materials, or plastics, in everyday use. Due to their wide range of properties and durability, plastic products are utilized in many industries and have a variety of applications. Some of the most common applications of plastics are in food packaging, textiles, transportation, and technology, to name a few. Because plastics have desirable properties such as low cost, light weight, and durability, they are preferred more than other materials in multiple applications. However, many of these polymeric materials are derived from petroleum, an industry that has caused irreparable damage to the environment. Petroleum is associated with increased greenhouse gas emissions, the destruction of ecosystems, and the pollution of fresh water and ground soil.[1] The carbon footprint of these materials will continue to put a strain on the environment as the demand increases.[2] To overcome these drawbacks but still take advantage of the convenience of plastics, it is necessary to take a green chemistry approach to

develop eco-friendly materials with comparable properties to traditional petroleum-based plastics. One way to achieve this is by utilizing bio-based renewable feedstocks as starting materials in the design of new polymers.

There are a variety of bio-based feedstocks that show promise as suitable replacements for petroleum. Vanillin, eugenol, and guaiacol are some of the main bio-based aromatic phenols with different functionalities that allow versatile modification.[3] Vanillin is the monoaromatic phenol with the highest availability that can be obtained as a byproduct of lignin waste.[4] The free hydroxyl and aldehyde functionalities of vanillin provide flexibility for the design of monomers to create polymeric materials[5], and has been used as a suitable replacement for petroleum derived monomers like bisphenol A (BPA)[6] and styrene.[7] Eugenol is another bio-based phenol that can be used to prepare monomers through different pathways and provides unique properties to polymers due to its allyl side chain. It is commonly found in clove; however, this constitutes a limited resource. A promising alternative strategy for obtaining eugenol, is the depolymerization of lignin which enables eugenol to be a viable bio-based resource.[8,9] Lastly, guaiacol is a phenol with a methoxy substituent at the ortho position. It is commonly found in shrubs, trees, clove oil, and is isolated from guaiacum. It is also a byproduct of the lignin industry which makes it attractive as a developing feedstock.[10] Because of the major concerns associated with petrochemicals, these bio-based monomers provide alternatives that can be explored to reduce the reliance on petroleum-based materials.

The use of renewable feedstocks is one way to reduce the carbon footprint of new materials, however, design efforts should also keep in mind the end of the product´s life. Recycling is a process of breaking down materials for the intent of being re-molded or re-shaped to be repurposed for additional use. Although still having some limitations regarding the infrastructure or loss of properties of the materials, recycling still constitutes a less resource intensive process than creating new materials.[11] A group of materials where recycling is of particular interest are thermosets. Traditional thermosets are highly crosslinked materials that lack the ability to be melted, remolded, or even less recycled.[12] An interesting way to overcome these limitations, is the use of dynamic covalent chemistry (DCC) to transform this set crosslinks into dynamic unions that can be broken and reformed with the use of external stimuli. DCC can therefore facilitate remolding, recycling, and even self-healing capabilities.[13–17] Among different exchangeable bonds, the dynamic transesterification between free hydroxyls and ester bonds has been the most explored dynamic chemistry.[18–26] The relatively high temperatures needed to trigger transesterification reactions (120-180°C) allows application of these materials at high temperatures without risking rigidity.[27]

3D printing technologies are of increasing interest, as they allow for reliable production of uniform products without the need for molds or machining in an efficient and cost-effective manner.[28,29] Vat polymerization (VP), a subset of 3DP, is a high-resolution manufacturing technique that uses liquid photoresins that polymerize

when irradiated with light. Common VP 3DP technologies are digital light projection (DLP) and stereolithography (SLA).

Transesterification reactions are very commonly used for designing VP printable vitrimers[27,30–32], and although more common in recent years, the reports thatadditionally take advantage of using bio-based feedstocks remain limited. Fei *et al.*[33 3434]reported a DLP printable resin formulation with ~62.5 to 68 wt% bio-based content from dimer acid. These materials showed self-healing and reprocessability due to dynamic transesterification reactions, and reported healing efficiencies of maximum 65%. Johnson *et al.*[34]reported a series of resins with up to 70 wt % bio-based content and functionalized lignin with excellent incorporation which still allowed them to be DLP printed. The reported materials possessed the ability to readily self-heal and be reprocessed through transesterification reactions. Additionally, an annealing treatment was performed which showed improvement of the mechanical performance, but the annealing effect in the thermosets is yet to be expanded upon.

With most manufacturing techniques, additional post processing treatments are required to optimize the performance of the materials. Heat treatments are among the most used postproduction methods to improve the mechanical properties of polymers. A particular heat treatment that has been explored for polymers is known as annealing.[35] Annealing consists of a heat treatment followed by a very slow cooling rate to allow rearrangement of the material´s microstructure into a more organized and stable configuration.[36] This heat treatment process can be used to rearrange a cross-linked polymer network since the polymer chains are able to move more freely with increased temperatures. This can be fine-tuned with different annealing times and higher annealing temperatures to result in polymers with specific mechanical properties. Buonerba *et al.*[37] reported increased elastic modulus of styrene/1-vinylfuran copolymers after undergoing annealing at 140 °C, confirming the increased cross-linking density of their materials. Studies on the effect of annealing on PLA and PLA blends have been done, showing increases in the fracture energy, Young´s modulus and tensile strength.[38,39] Additional reports studying the effect of annealing on polyphenylene sulfide fiber composites also indicate increases of the modulus values.[40] There are reports on the effect of annealing in vitrimers, showing that it can influence the connectivity in dynamically crosslinked vinylogous urethanes,[41] and more recently, the result of annealing VP-printed urethane acrylate networks was explored, showing it improves the self-healing between the printed layers.[42] The effect of annealing in the mechanical performance of bio-based VP-printed transesterification vitrimers, and the relationship of the behaviors with the structures is yet to be explored. Here, we report a series of completely bio-based, self-healable, and reprocessable VP-printed thermosets based on transesterification exchange reactions. Vanillin, eugenol and guaiacol were chosen as the bio-based feedstocks as these all possess a reactive phenol and vary only on the para-hydroxy side chains. These particular structural

variables could provide some insight on the structure-property relationships with the effects of annealing.

## *Materials and methods*

### Materials

All chemicals were used as received unless otherwise noted. Vanillin (99%), Eugenol and Guaiacol were purchased from Alfa Aesar. Triethylamine (TEA), sodium chloride (NaCl) sodium bicarbonate ($NaHCO_3$), hydrochloric acid (HCl), sodium hydroxide (NaOH), dichloromethane (DCM), and tetrahydrofuran (THF) were purchased from Fisher Scientific. Acrylic acid and zinc acetylacetonate ($Zn(acac)_2$) were purchased from Sigma-Aldrich. (+/-) Epichlorohydrin was purchased from ACROS organics. Benzyltriethylammonium Bromide 98.0+% (TEBAC) and Diphenyl-(2,4,6-trimethylbenzoyl) phosphine oxide (TPO) were purchased from TCI America.

### Synthetic procedures

### Vanillin glycidyl ether (VGE)

Vanillin glycidyl ether (VGE) was synthesized according to previously reported procedures and slightly adapted to our laboratory practices. [43–45] Vanillin (20 g, 0.13 mol) and epichlorohydrin (323.5 g, 3.5 mol), were added to a two necked round bottom flask equipped with a condenser and magnetic stirring. Benzyltriethylammonium chloride (TEBAC) (3 g, 0.013 mol) was added as the phase transfer catalyst and the mixture was refluxed at 85 °C for 3 h under stirring. The reaction mixture was then cooled to room temperature and 41.15 mL of a 20 % w/w NaOH aqueous solution was added dropwise. After stirring the reaction mixture at room temperature overnight, the flask was introduced with ethyl acetate and filtered to remove formed NaCl. The organic phase was washed three times with water, brine, and dried over anhydrous $Na_2SO_4$. After condensation of the solvent by rotary evaporation, a light-yellow solid was obtained in an 85% yield and used with no further purification ($^1$H NMR Figure S1).

### Eugenol glycidyl ether (EGE)

Eugenol glycidyl ether (EGE) was synthesized following a previously reported procedure.[46,47] Eugenol (32.6 g, 0.2 mol), epichlorohydrin (116 g, 1.2 mol) and TEBAC (3.6 g, 0.016 mol) as the phase transfer catalyst, were added to a 250 mL round bottom flask equipped with a condenser and magnetic stirring. The mixture was refluxed at 100 °C for one hour. After cooling to room temperature, 112.5 mL of a 20 % w/w NaOH aqueous solution with TEBAC (3.6 g, 0.016 mol) was added dropwise and maintained under stirring for 1.5 h. The reaction mixture was then diluted with 50 mL of ethyl acetate, and the organic phase was washed three times with water, brine, and dried over anhydrous $Na_2SO_4$. The solvent was removed by rotary evaporation and the product was obtained as a light-yellow oil in a 90% yield and used without further purification ($^1$H NMR Figure S2).

### Guaiacol glycidyl ether (GuGE)

Guaiacol glycidyl ether (GuGE) was synthesized following the procedure used for the synthesis of EGE. Guaiacol (20 g, 0.16 mol), epichlorohydrin (94 g, 1 mol) and TEBAC (2.2 g, 0.01 mol) as the phase transfer catalyst, were added to a 250 mL round bottom flask equipped with a condenser and magnetic stirring. The mixture was refluxed at 100 °C for one hour. After cooling to room temperature, 90 mL of a 20 % w/w NaOH aqueous solution with TEBAC (2.2 g, 0.01 mol) was added dropwise and maintained under stirring for 1.5 h. The reaction mixture was then diluted with 50 mL of ethyl acetate, and the organic phase was washed three times with water, brine, and dried over anhydrous $Na_2SO_4$. The solvent was removed by rotary evaporation and the product was obtained as a white solid in an 80% yield and used without further purification ($^1$H NMR Figure S3).

### Vanillyl alcohol

Vanillyl alcohol was synthesized by the reduction of vanillin with sodium borohydride ($NaBH_4$) according to the following procedure. Vanillin (20 g, 0.13 mol) was added to a round bottom flask and dissolved in 40 mL of ethanol. The flask was put in an ice bath and a solution of $NaBH_4$ (5 g, 0.13 mol) dissolved in 38 mL of 1M NaOH, was added dropwise over a period of 10 minutes. When the addition was complete, the reaction was stirred at room temperature for 10 min and then placed once again in the ice bath. To decompose the remaining $NaBH_4$, around 40 mL of aqueous 6M HCl were added dropwise until evolution of $H_2$ stopped. The pH was confirmed acidic, and cooling allowed precipitation of the product as a white solid with quantitative yield and use with no further purification ($^1$H NMR Figure S4).

### Diglycidyl ether of vanillyl alcohol (DGEVA)

Diglycidyl ether of vanillyl alcohol (DGEVA) was synthesized according to a previously reported procedure.[6] Vanillyl alcohol (10 g, 0.06 mol), epichlorohydrin (60 g, 0.65 mol) and TEBAC (1.5 g, 0.006 mol) as the phase transfer catalyst, were added into a round bottom flask and stirred for 4 h at room temperature. The reaction mixture was cooled to 0 °C with the use of an ice bath, followed by the dropwise addition of 80 mL of a 33 % w/w NaOH aqueous solution under vigorous stirring. After stirring the reaction mixture overnight, the flask was introduced with 250 mL of water, and extracted three times with ethyl acetate. The organic phases were combined, washed with brine, and dried over anhydrous $Na_2SO_4$. The solvent was removed by rotary evaporation to obtain a pale-yellow solid in an 80 % yield and used without further purification ($^1$H NMR Figure S5).

### Vanillin glycidyl ether acrylate (VGEA) [48,49], eugenol glycidyl ether acrylate (EGEA)[50], guaiacol glycidyl ether acrylate (GuGEA)[51], and diglycidyl ether vanillin diacrylate (DGEVDA)

The synthesis of the acrylated crosslinker and monomers was carried out based on a similar procedure found in literature for the opening of epoxides with methacrylic acid[52] and modified accordingly for each monomer/crosslinker epoxy precursor. A generalized version of the synthetic procedures is the following. The epoxy/diepoxy precursor was added to a round bottom flask with acrylic acid (21 eq.) as both reagent and solvent. BHT (0.02eq. to acrylic acid) was added as an inhibitor, and the mixture was kept under a $N_2$ atmosphere. Triethylamine (0.036 eq.) was injected through a syringe and the reaction mixture was heated to 100 °C and kept under reflux for 4 h. After cooling to room temperature, the flask was introduced with ethyl acetate, washed with $NaHCO_3$ (sat. aq.), brine, and dried over anhydrous $Na_2SO_4$. The resulting acrylated monomers were purified through column chromatography with hexane:ethyl acetate at 6:4, 7:3, and 3:7 ratios for VGEA, EGEA and GuGEA respectively and characterized by $^{1}H$ and $^{13}C$ NMR.ESI-MS analysis of the acrylated monomers and crosslinker can also be found in the SI (Figures S6-S17).

**Electrospray Ionisation Mass Spectrometry (ESI-MS)**

Synthesized materials were characterized with an Agilent 1290 Infinity II LC/MSD iQ system. A method of 5-95% MS grade acetonitrile in DI $H_2O$ (both containing 0.1% formic acid) was used with a flow of 1 mL/min. Spectra obtained with Agilent OpenLab CDS software.

**Resin formulation and 3D printing**

The first set of resin formulations were based on experimental mixtures of VGEA as the monomer and varied molar concentrations (5, 10, 20, 30, and 40 mol%) of DGEVDA as the crosslinker. The 80 mol% VGEA and 20 mol% DGEVDA formulation exhibited the best printability and self-healing behavior, therefore 20 mol% of DGEVDA was chosen as the crosslinker for the EGEA and GuGEA formulations. Dynamic transesterification reactions (DTERs) are known to require a catalyst to occur effectively,[27] therefore in all these formulations we included 5 mol% zinc acetylacetonate relative to the hydroxy groups. TPO was chosen as the photoinitiator and added to all formulations (2 wt.%). The resins were prepared in an abler vial, by directly weighing the previously calculated monomer (80 mol%) and crosslinker (20 mol%) amounts. Then, the catalyst was weighted and added to the vial, followed by heating with a heat gun to ensure full dissolution of the catalyst. The photoinitiator was weighted and added last, and the resins were ultrasonicated for 30 min to fully incorporate the photoinitiator, as well as to avoid air bubbles while printing. After this, the resins were slightly warmed with a heat gun to facilitate the flow out of the container, into the vat of the Photon Zero DLP 3D printer. Specimens for tensile testing, and lattices were all printed keeping the printing parameters consistent. The raising speed was set to 3 mm/s and the exposure time per layer was set to 60 s. The prints were washed twice with isopropanol, the first time to remove excess unreacted resin, and the second one while sonicating for 5 min to remove additional

unreacted material within the networks, followed by 24 h post-curing under a 405 nm lamp.

### Annealing of the samples

Annealing is the heat treatment of a material for extended periods of time, in which the cooling rate is kept the slowest possible, such that the equilibrium microstructure is achieved.[36,39] This treatment of polymeric materials has shown influence in the chain mobility and improvement of the mechanical performance.[35,38] Annealing of the printed thermosets was performed in an oven at 80°C for 12 h. After this time the oven was turned off and left to cool to room temperature with the samples inside and without opening the oven door to allow for slow cooling.

### Gel content and swelling experiments

Gel content and swelling experiments were carried out for both as printed and annealed samples to ensure complete incorporation of the components into the thermoset polymer network. The solvents used were toluene, tetrahydrofuran, water, and ethanol. The experiments were done in triplicate and the average and standard deviation are reported (Figures S22-S25).

### Fourier transform infrared spectroscopy (FT-IR)

Infrared spectra were obtained with an attenuated total reflection (ATR) accessory coupled to a Fourier transform infrared (FT-IR) spectrometer (Cary 600 Series). All spectra were recorded in the 4000−400 $cm^{-1}$ range with a resolution of 2 $cm^{-1}$, accumulating 32 scans.

### Tensile testing

Uniaxial tensile testing to failure of ASTM D638 standard type V specimens was performed using an Instron 5500A testing machine with a 1 kN load cell at a rate of 5 mm/min until failure.

### Compression testing

Uniaxial compression testing was performed using an Instron 6800 universal testing machine with a 50 kN load cell for 3D printed and reprocessed cylindrical compression samples (10 mm diameter x 10 mm height). The samples tested consisted of as printed, annealed, and reprocessed samples. All compression tests of these samples were conducted at room temperature using a crosshead rate of 10 mm/min until specimen failure.

### Thermogravimetric analysis (TGA)

TGA of 5-10 mg samples loaded into an alumina crucible, was conducted from 25 to 700 °C at a heating rate of 10 °C/min, under a $N_2$ atmosphere with a flow rate of 100 mL/min using a Mettler Toledo SDT.

### Differential scanning calorimetry (DSC)

DSC curves were obtained on a TA Instruments DSC Q2000 equipped with an air-fin cooler. The measurements were conducted under a $N_2$ atmosphere, with a 20 mL/min flow rate. Approximately 5 to 10 mg of each sample were placed in Tzero Aluminum Hermetic pans. The heating rate was 10 °C/min and the samples were subjected to three heating/cooling cycles from -40 to 200 °C. The data from the second cycle was selected for all experiments.

### Self-Healing experiments

For the self-healing experiments, a small piece of the printed specimen of each formulation was gently scratched using a razor blade. Optical microscopy images were obtained for each scratched specimen as the “before healing” pictures, and then were placed in between two glass slides, and held together with two binder clips to apply pressure. The chosen temperatures for the healing experiments were 120 and 180°C as these are known to promote transesterification reactions.[27] The cut samples were placed in an oven for 16 h, and optical microscopy images were obtained to evaluate the healing of each formulation. These tests were carried out in triplicate to ensure reproducibility.

### Reprocessing

To evaluate the reprocessability of the samples, the printed specimens were ground into small pieces through mechanical grinding, then placed into a metallic mold and compressed under 1500 psi at 140 °C for 4h using a Carver hydraulic hot-press.

## *Results and discussion*

### Synthesis of components and photo-resin formulation for 3D printing

A general synthetic scheme for the preparation of the monomers and crosslinker is illustrated in Scheme 1. The design of the resin components was executed with the intention that the resulting thermosets possessed the ability to self-heal and be recycled with the use of DTERs. Previous reports show that the presence of free hydroxy groups allows the networks to undergo transesterification reactions.[24,25,53] Additionally, the abundance of ester functionalities throughout the polymer networks, can influence the relaxation times, allowing fast topology rearrangements.[25] Based on this, the monomers and crosslinker ought to possess beta hydroxy ester moieties. All the resin components were functionalized with acrylate moieties through the ring-opening reaction of the epoxides with acrylic acid. This synthetic pathway provides the photo-reactive moieties for the polymerization, along with a free hydroxy moiety in the beta position for the DTERs.

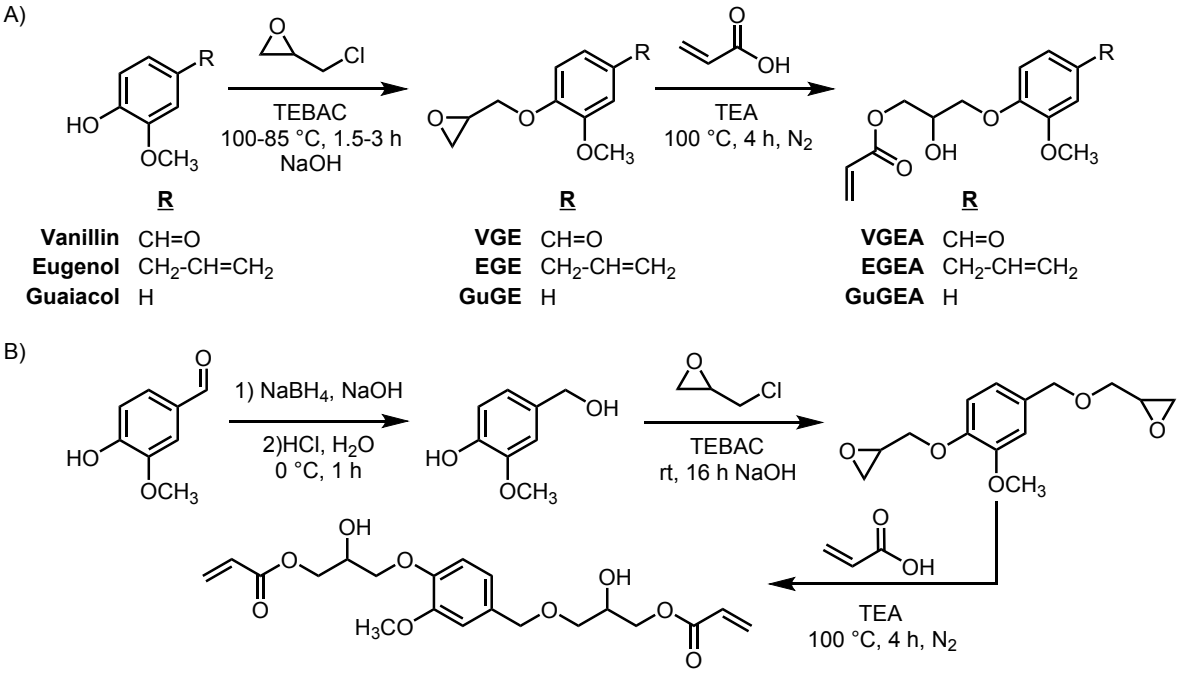


**Scheme 1.** General synthesis of the acrylated A) monomers and B) crosslinker.

The resin formulations were prepared as mentioned in the methods section. Based on the good healing performance of the 80 mol% VGEA and 20 mol% DGEVDA (VGEA+20DGEVDA) formulation, a 20 mol% crosslinker concentration was chosen for the remaining monomers (Figure S28). All 20 mol% formulations exhibited excellent printability and the comparison of the printed lattices can be seen in figure 1. The GuGEA+20DGEVDA formulation showed the best printing accuracy as seen from the smoother edges with less layer visibility. We hypothesize this could be owing to the lack of sidechains which results in a relative higher abundance of reactive acrylate moieties per mol of monomer, possibly resulting in a slightly faster rate of polymerization. Additionally, the absence of sidechains in GuGEA, reduces the possibility of side reactions, dimerization or degradation like in the case of VGEA which could compromise the reactivity and printing efficiency. Additionally, the VGEA+20DGEVDA thermoset presented significant yellowing after post-curing which became more evident after annealing. The EGEA+20DGEVDA thermoset presented very light yellowing and the GuGEA+20DGEVDA thermoset presented no visible yellowing, even after the annealing treatment. We hypothesize that the yellowing observed behavior between the three monomers might be attributed to crosslinking between the aromatic rings due the formation of radicals during the photopolymerization. Vanillin is known to undergo facile triplate-mediated photodegradation, that leads to vanillin dimers and possible oligomers. [54] This previously reported evidence could explain the significantly more evident yellowing and lower printing accuracy of the VGEA formulations. [54]

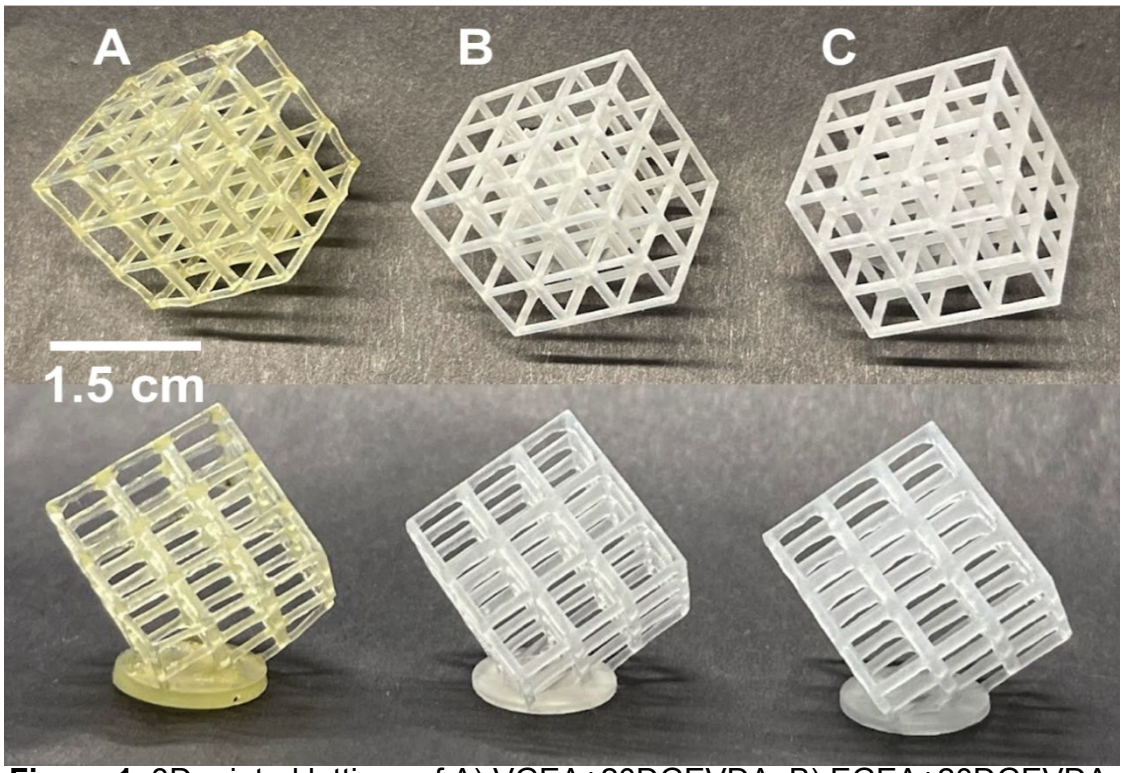


**Figure 1.** 3D printed lattices of A) VGEA+20DGEVDA, B) EGEA+20DGEVDA and C) GuGEA+20DGEVDA.

**Structural characterization**

The structure of the synthesized monomers and crosslinkers was confirmed by $^{1}H$ NMR (Figures S1-S9). The resins and the printed thermosets were analyzed through FT-IR spectroscopy (Figures S10-S13), mainly to confirm the presence of the C=O (~1720 $cm^{-1}$) and -OH (~3400-3450 $cm^{-1}$) moieties. Additionally, comparing the spectra of the resin vs the polymers, the disappearance of the C=C (~810, 1405 and 1640 $cm^{-1}$) signals and increase in the C-H (2868 and 2952 $cm^{-1}$) signals indicated complete polymerization.[55] These characteristic peaks of the polymerization were highly noticeable when comparing the resin spectrum to the as printed spectrum. However, when comparing the as printed spectrum to the annealed spectrum, not much change was observed. This could be a good indication of the already complete polymerization before annealing. One more evident difference between the resin, as printed and annealed spectra, was the continuous broadening and shifting of the -OH (~3400-3450 $cm^{-1}$) signal. This might indicate a higher amount of hydrogen bonded -OH groups, as well as increased relaxation of the -OH excited vibrational state.[56] To further confirm the incorporation of the components into the network, gel content and swelling experiments were conducted. The results from these

experiments are provided in figures S14-S17, and the gel content percentages of all formulations are mostly above 85%, which indicates high crosslinking and good network incorporation. When comparing the as printed and annealed samples, we observe that the annealed samples lead to higher gel content percentages. Based on these results it could be suggested that annealing increases the crosslinking or chain entanglement in the networks. However, since the FT-IR results show no significant change in the C=C signals, we hypothesize that the increase in crosslinking could be caused by improved physical crosslinking interactions such as hydrogen bonding between the free hydroxyl groups and myriad hydrogen bond acceptors in the polymer network resulting in the creation of additional crystalline domains. This hypothesis is supported by the changes in the -OH signal in the FT-IR spectra, which broaden with annealing suggesting a higher number of hydroxyl groups involved in hydrogen bonding (Figures S18-S21).

## Thermal characterization of the thermosets

TGA and DSC curves of the varied ratios of VGEA+DGEVDA thermosets are provided in Figure S26. From these data we can observe that the glass transition temperature ($T_g$) increases with higher crosslinker concentration. The thermal characterization of the 20 mol% DGEVDA thermosets of VGEA, EGEA and GuGEA can be seen in Figure 2.

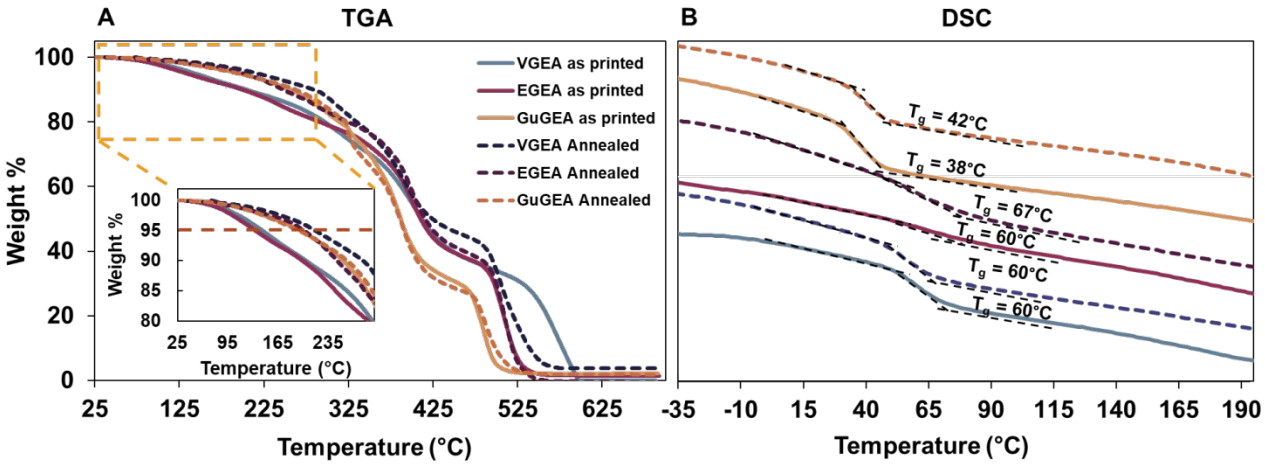


| C | -5 weight % (°C) | | Glass Transition (°C) | |
|---|---|---|---|---|
| | As Printed | Annealed | As Printed | Annealed |
| VGEA+20mol%DGEVDA | 143 | 218 | 60 | 60 |
| EGEA+20mol%DGEVDA | 134 | 202 | 60 | 67 |
| GuGEA+20mol%DGEVDA | 196 | 195 | 38 | 42 |

**Figure 2.** Thermal characterization of the as printed (solid) and annealed (dashed) VGEA, EGEA and GuGEA +20DGEVDA formulations. A) TGAs showing the 5 weight % loss temperature. B) DSCs showing the $T_g$s. C) Table summarizing the temperature values.

When comparing the temperatures of 5 wt % loss of the as printed samples, we observe that EGEA has the lowest value, followed by VGEA and the highest value is that of GuGEA. The TGAs of the annealed samples show an increase in the 5 weight % loss temperature of the VGEA and EGEA formulations but show no change for the GuGEA. For the VGEA and EGEA formulations this change could be attributed to an increase in the hydrogen bonding and chain rearrangement in the thermoset networks due to the annealing treatment. However, in the case of the GuGEA formulation, due to the lack of sidechains in this monomer there is no added potential for hydrogen bonding or chain rearrangement which results in no change in the 5 weight % loss temperature.

**Mechanical properties**

The mechanical properties were analyzed through tensile testing experiments of at least three specimens per formulation. For the varied VGEA+DGEVDA ratio thermosets, the general observation was that, as the amount of crosslinker increased, the materials became stiffer, losing strain % but with increased Young´s modulus and ultimate tensile strength (Figure S27). The stress-strain curve of the different monomers with 20 mol% DGEVDA, is shown in figure 3A. When comparing the results of the as printed specimens of the three different monomers, we can note that EGEA gives the strongest material with the highest Young´s modulus and UTS. GuGEA is situated somewhat in the middle and VGEA gives the softest material with the lowest Young´s modulus and UTS, but the highest strain at break.

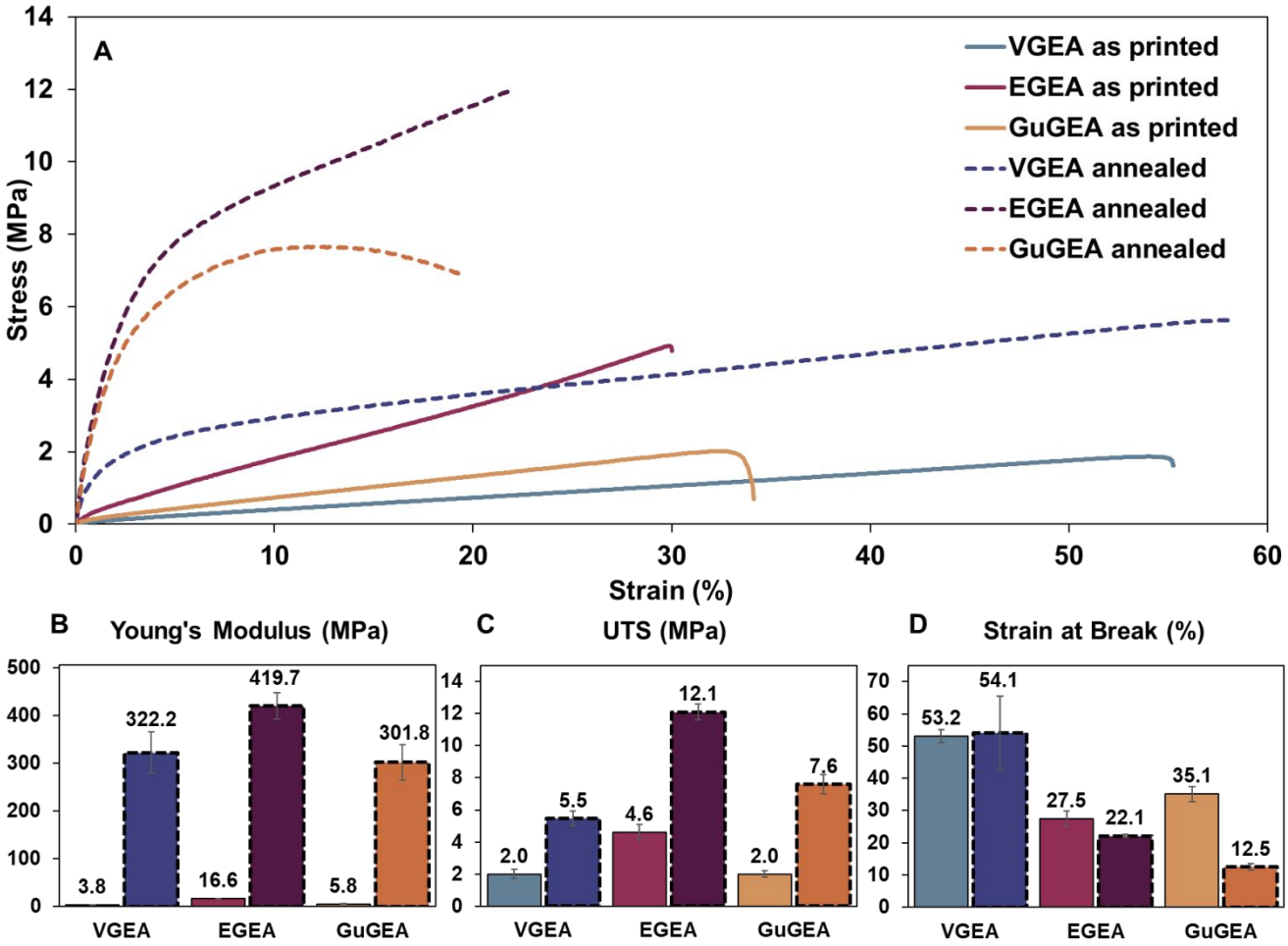


**Figure 3.** A) Stress-strain plot of as printed (solid) and annealed (dashed) samples. Bar plot comparison of the mechanical properties B) Young's modulus, C) UTS and D) Strain at break of the VGEA, EGEA and GuGEA plus 20mol% DGEVDA thermosets.

## Effect of annealing on the mechanical performance

Representative stress-strain curves of the annealed specimens are also provided, and bar plots for comparing the change of the properties after the annealing treatment can be seen in figure 3B, C and D. As a general trend, the annealing treatment significantly increased the Young´s modulus by ~ 8500 %, 2500 % and, 5100 % for VGEA, EGEA and GuGEA respectively. Additionally, the UTS also improved after annealing by ~ 170 %, 160 % and 280 %. The strain at break shows a small reduction for the three monomer formulations, with GuGEA showing the greatest decrease. These results are consistent with the effects of annealing reported in literature, and the data described supports the conclusion that annealing strengthens the structure of the polymer, by increasing the crystallinity, therefore resulting in higher Young´s modulus and UTS but decreasing the strain at break.[38,39] In an attempt to elucidate the structure/property relationship of the different

monomers, we hypothesize the following. Annealing increases the crystallinity of the material by increasing the number of hard segments due to an increase in hydrogen bonding interactions, supported by the FT-IR results discussed in the structural characterization section (Figures S18-S21).[57] Additionally, VGEA thermosets exhibit a more dramatic increase in the Young´s modulus which can be also explained by the ability of the aldehyde side chain to participate in hydrogen bonding therefore increasing the stiffness. In the case of the UTS, GuGEA thermosets exhibit the largest increase after annealing, which could be explained by the lack of side chains in the aromatic monomer, which allow more tightly packing of the networks in the crystalline regions, resulting in a stronger material with lower elongation (Figure 3).

**Self-healing and reprocessing**

As mentioned in the synthesis discussion, the monomers and crosslinker contain free hydroxy moieties which allow DTERs to happen. Additionally, the formulations contain a 5 mol% concentration of $Zn(acac)_2$ which activates the ester carbonyl for DTERs. The healing ability of the different monomers with 20 mol% DGEVDA are demonstrated in Figure 4. VGEA and EGEA thermosets exhibit excellent healing capabilities, as seen from the complete vanishing of the inflicted surface defects. The GuGEA thermoset also shows the ability to heal the scratch, however a very faint scar can still be observed even after the 180 °C treatment. As mentioned before, the lack of side chains in the GuGEA monomer might contribute to tighter packing in the polymer networks, reducing the potential for chain rearrangement and therefore resulting in some leftover scarring (Figure S29).

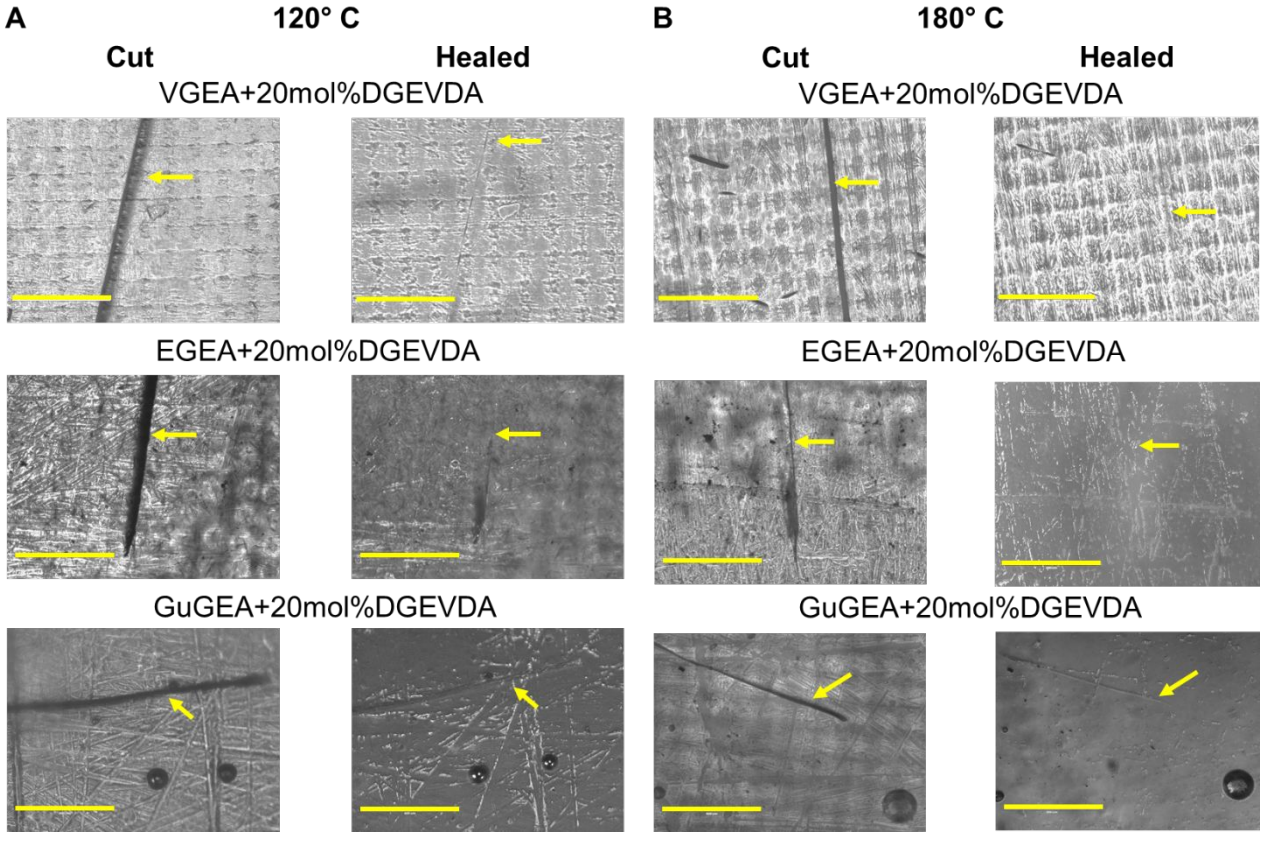

**Figure 4.** Optical microscopy images (scale bar 400 μm) of the scratches on the sample surface and the results after the heat treatment at A) 120 °C and B) 180 °C for 16 h.

Remolding experiments of the 20 mol% DGEVDA thermosets were performed to explore the reprocessing ability of the materials. Only VGEA+20DGEVDA showed complete incorporation of the pieces into the new form at 140 °C and 1500 psi for 4 h, using a cylindrical mold (Figure S30). The new cylinder shapes of reprocessed VGEA+20DGEVDA, were compression tested and compared to the as printed and annealed samples (Figure 5). Compared to the original properties of the as printed samples, the reprocessed cylinders show recoveries of 957%, 75% and 93% of the Young´s modulus, compressive strength, and strain at break respectively. These high recovery percentages, indicate that this thermoset formulation has the ability to be recycled without compromising its mechanical performance. Additional reprocessing experiments for the remaining monomer formulations were conducted at extended times (24 h) into a flat disc and better incorporations were observed. The pictures for these experiments can be seen in Figure S31.

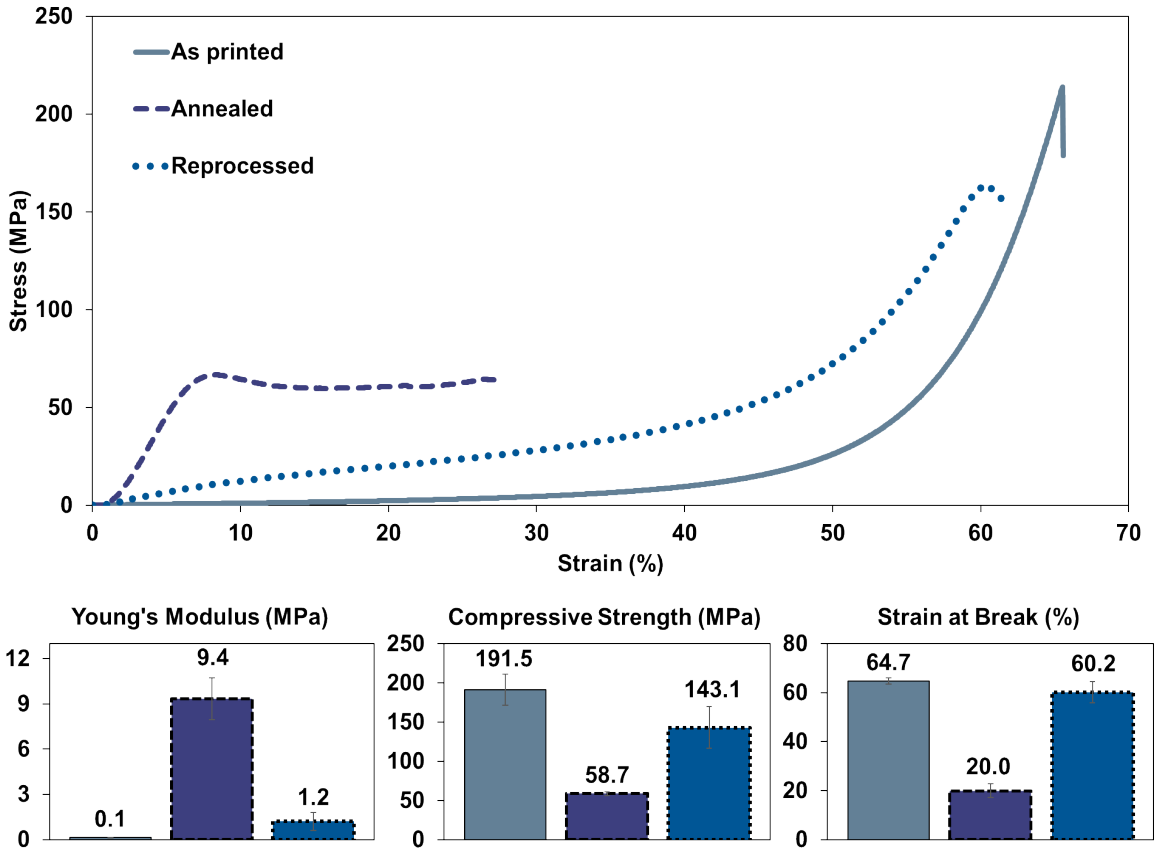

**Figure 5.** Comparison of compression curves and properties of as printed (solid), annealed (dashed) and reprocessed (dotted) samples for VGEA+20DGEVDA.

## Conclusion

In this work, three different bio-based monomers derived from vanillin, eugenol and guaiacol, were synthesized and formulated into photo printable resins with DGEVDA as a bio-based crosslinker. These polymer formulations contained significantly high bio-based content since the synthesis of all components was derived from renewable materials. Additionally, based on the synthetic design, these thermosets have the potential to be nearly 100% bio-based in the future, since it has been reported both epichlorohydrin,[58] and acrylic acid,[59,60] can be produced sustainably from biobased sources. The resulting thermosets possessed beta hydroxy ester moieties which enabled the DTERs that provided self-healing and reprocessability to the materials. A post printing annealing treatment was given to the thermosets and the effects on the structural, thermal, and mechanical properties were discussed. Annealing dramatically increased the Young´s modulus and UTS, providing these thermosets with superior mechanical perfrormance to previously reported bio-based materials.[33,34] Further optimization of the reprocessing parameters is to be explored to quantify the reprocessability of the three thermoset formulations. Additionally, the abundance of ester moieties could allow exploration of chemical degradability to strive for full recyclability through chemical recycling.

## Associated content

Supporting Information

$^{1}$H NMR and $^{13}$C NMR spectra of synthesized monomers and crosslinker; FTIR spectra of resin formulations; Gel content experiments of formulations in water and ethanol; Strain−stress plot of compression tests of all formulations; Comparison of compression tests of printed, annealed, and reprocessed samples are included in the Supporting Information.

## Author information

Corresponding Author

Ronald A. Smaldone − Department of Chemistry and Biochemistry, Department of Materials Science and Engineering, University of Texas at Dallas, Richardson, Texas 75080, United States; orcid.org/0000-0003-4560-7079
Email: ronald.smaldone@utdallas.edu

Authors

Karen P. Cortés-Guzmán−Department of Chemistry and Biochemistry, University of Texas at Dallas, Richardson, Texas 75080, United States; orcid.org/0000-0002-8793-4687

Ankit R. Parikh − Department of Mechanical Engineering, University of Texas at Dallas, Richardson, Texas 75080, United States; orcid.org/0000-0003-0107-5533

Marissa L. Sparacin − Department of Chemistry and Biochemistry, University of Texas at Dallas, Richardson, Texas 75080, United States; orcid.org/0000-0003-2500-8239

Rebecca M. Johnson − Department of Chemistry and Biochemistry, University of Texas at Dallas, Richardson, Texas 75080, United States; orcid.org/000-0002-7560-4672

Walter E. Voit − Department of Materials Science and Engineering, Department of Mechanical Engineering, The University of Texas at Dallas, 800 W Campbell Road, Richardson, Texas 75080, United States; orcid.org/0000-0003-0135-0531

Lauren Adegoke − Department of Biomedical Engineering, University of North Texas, Denton, Texas 75203, United States; orcid.org/0000-0001-8513-4160

Melanie Ecker − Department of Biomedical Engineering, University of North Texas, Denton, Texas 75203, United States; orcid.org/0000-0002-0603-6683

Notes

The authors declare no competing financial interest.

**Author Contributions**

The manuscript was written through contributions of all authors. All authors have given approval to the final version of the manuscript.

**Conflicts of interest**

The authors declare no conflicts of interest.

**Acknowledgments**

We acknowledge Laurel M. Hagge from the Department of Chemistry and Biochemistry and Ramyapriya Krishnasamy from the Advanced Polymer Research Lab (APRL) at UT Dallas for performing mass spectrometry and surface measurements.

**Funding Sources**

K.C.G. acknowledges the Consejo Nacional de Ciencia y Tecnología (CONACYT, Mexican Council of Science and Technology) for doctoral fellowship. We also

acknowledge the Advanced Polymer Research Lab (APRL) at UT Dallas for access to facilities for the thermal characterization of polymers. UT Dallas. A.K.P. acknowledges scientific and internship support from the U.S. Food and Drug Administration. R.A.S. acknowledges support from UT Dallas, and the Army Research Laboratory (W911SR-22-C-0048)

## References

1 W. Bach, *FOSSIL FUEL RESOURCES AND THEIR IMPACTS ON ENVIRONMENT AND CLIMATE**, vol. 6.

2 K. G. Harding, J. S. Dennis, H. von Blottnitz and S. T. L. Harrison, *J Biotechnol*, 2007, **130**, 57–66.

3 R. Ding, Y. Du, R. B. Goncalves, L. F. Francis and T. M. Reineke, *Polym Chem*, 2019, **10**, 1067–1077.

4 M. Fache, B. Boutevin and S. Caillol, *ACS Sustain Chem Eng*, 2016, **4**, 35–46.

5 M. Fache, E. Darroman, V. Besse, R. Auvergne, S. Caillol and B. Boutevin, *Green Chem.*, 2014, **16**, 1987–1998.

6 M. Fache, R. Auvergne, B. Boutevin and S. Caillol, *Eur Polym J*, 2015, **67**, 527–538.

7 J. F. Stanzione, J. M. Sadler, J. J. La Scala, K. H. Reno and R. P. Wool, *Green Chem.*, 2012, **14**, 2346–2352.

8 V. V. Kouznetsov and L. Y. Vargas Méndez, *J Appl Polym Sci*, 2022, 139.

9 S. Caillol, B. Boutevin and R. Auvergne, *Polymer (Guildf)*, 2021, **223**, 123663.

10 S. Zhao, X. Huang, A. J. Whelton and M. M. Abu-Omar, *ACS Sustain Chem Eng*, 2018, **6**, 7600–7608.

11 D. E. Fagnani, J. L. Tami, G. Copley, M. N. Clemons, Y. D. Y. L. Getzler and A. J. McNeil, *ACS Macro Lett*, 2021, 10, 41–53.

12 Y. Jin, Z. Lei, P. Taynton, S. Huang and W. Zhang, *Matter*, 2019, 1, 1456–1493.

13 M. Podgórski, B. D. Fairbanks, B. E. Kirkpatrick, M. McBride, A. Martinez, A. Dobson, N. J. Bongiardina and C. N. Bowman, *Adv. Mater.*, 2020, **32**, 1–26.

14 J. Dahlke, S. Zechel, M. D. Hager and U. S. Schubert, *Adv Mater Interfaces*, 2018, **5**, 1800051.

15 K. Imato, A. Takahara and H. Otsuka, *Macromolecules*, 2015, **48**, 5632–5639.

16 A. Durand-Silva, K. P. Cortés-Guzmán, R. M. Johnson, S. D. Perera, S. D. Diwakara and R. A. Smaldone, *ACS Macro Lett*, 2021, **10**, 486–491.

17 K. P. Cortés-Guzmán, A. R. Parikh, M. L. Sparacin, A. K. Remy, L. Adegoke, C. Chitrakar, M. Ecker, W. E. Voit and R. A. Smaldone, *ACS Sustain Chem Eng*, 2022, **10**, 13091–13099.

18 M. Capelot, D. Montarnal, F. Tournilhac and L. Leibler, *J Am Chem Soc*, 2012, **134**, 7664–7667.

19 F. I. Altuna, C. E. Hoppe and R. J. J. Williams, *Eur Polym J*, 2019, **113**, 297–304.

20 M. Chen, L. Zhou, Y. Wu, X. Zhao and Y. Zhang, *ACS Macro Lett*, 2019, **8**, 255–260.

21 A. Demongeot, R. Groote, H. Goossens, T. Hoeks, F. Tournilhac and L. Leibler, *Macromolecules*, 2017, **50**, 6117–6127.

22 K. Yu, P. Taynton, W. Zhang, M. L. Dunn and H. J. Qi, *RSC Adv*, 2014, **4**, 48682–48690.

23 F. I. Altuna, V. Pettarin and R. J. J. Williams, *Green Chem.*, 2013, **15**, 3360–3366.

24 D. Montarnal, M. Capelot, F. Tournilhac and L. Leibler, *Science*, 2011, **334**, 965–968.

25 W. Denissen, J. M. Winne and F. E. du Prez, *Chem Sci*, 2016, **7**, 30–38.

26 J. Wu, X. Yu, H. Zhang, J. Guo, J. Hu and M.-H. Li, *ACS Sustain Chem Eng*, 2020, **8**, 6479–6487.

27 T. Liu, B. Zhao and J. Zhang, *Polymer,* 2020, **194**, 122392.

28 B. Berman, *Bus Horiz*, 2012, **55**, 155–162.

29 J. W. Stansbury and M. J. Idacavage, *Dent. Mater.*, 2016, **32**, 54–64.

30 G. M. Scheutz, J. J. Lessard, M. B. Sims and B. S. Sumerlin, *J Am Chem Soc*, 2019, **141**, 16181–16196.

31 Q. Shi, K. Yu, X. Kuang, X. Mu, C. K. Dunn, M. L. Dunn, T. Wang and H. J. Qi, *Mater Horiz*, 2017, **4**, 598–607.

32 H. Gao, Y. Sun, M. Wang, Z. Wang, G. Han, L. Jin, P. Lin, Y. Xia and K. Zhang, *ACS Appl Mater Interfaces*, 2021, **13**, 1581–1591.

33 M. Fei, T. Liu, B. Zhao, A. Otero, Y.-C. Chang and J. Zhang, *ACS Appl Polym Mater*, 2021, **3**, 2470–2479.

34 R. M. Johnson, K. P. Cortés-Guzmán, S. D. Perera, A. R. Parikh, V. Ganesh, W. E. Voit and R. A. Smaldone, *J. Polym. Sci.* 2023, **1.**

35 G. S. Y. Yeh, R. Hosemann and J. Loboda-C, *Annealing effects of polymers and their underlying molecular mechanisms**, 1976.

36 M. K. Banerjee, in *Comprehensive Materials Finishing*, Elsevier Inc., 2017, vol. 2–3, pp. 1–49.

37 A. Buonerba, V. Speranza, C. Capacchione, S. Milione and A. Grassi, *Eur Polym J*, 2018, **99**, 368–377.

38 T. Takayama, M. Todo and H. Tsuji, *J Mech Behav Biomed Mater*, 2011, **4**, 255–260.

39 T. Gy and Y. Ikada, *Properties and morphologies of poly(L-lactide): 1. Annealing condition effects on properties and morphologies of poly(L-lactide)*, 1995, vol. 36.

40 F. Y. C. Boey, T. H. Lee and C. Y. Yue, *Annealing Effects on the Dynamic Mechanical Properties of Aromatic Polyphenylene Sulphide Fibre Reinforced Composite*, 1991, vol. 10.

41 J. S. A. Ishibashi, I. C. Pierce, A. B. Chang, A. Zografos, B. M. El-Zaatari, Y. Fang, S. J. Weigand, F. S. Bates and J. A. Kalow, *Macromolecules*, 2021, **54**, 3972–3986.

42 L. S. Hamachi, D. A. Rau, C. B. Arrington, D. T. Sheppard, D. J. Fortman, T. E. Long, C. B. Williams and W. R. Dichtel, *ACS Appl Mater Interfaces*, 2021, **13**, 38680–38687.

43 M. Fache, B. Boutevin and S. Caillol, *Green Chem.*, 2016, **18**, 712–725.

44 Q. Yu, X. Peng, Y. Wang, H. Geng, A. Xu, X. Zhang, W. Xu and D. Ye, *Eur Polym J*, 2019, **117**, 55–63.

45 C. Aouf, C. le Guernevé, S. Caillol and H. Fulcrand, *Tetrahedron*, 2013, **69**, 1345–1353.

46 B. Liu, J. Chen, N. Liu, H. Ding, X. Wu, B. Dai and I. Kim, *Green Chem.*, 2020, **22**, 5742–5750.

47 C. Li, H. Fan, T. Aziz, C. Bittencourt, L. Wu, D.-Y. Wang and P. Dubois, *ACS Sustain Chem Eng*, 2018, **6**, 8856–8867.

48 H. Akiko; O. Yoshihiko; A. Masato; N. Fumiaki. Japan, JP2000109501, 2000-04-18.

49 M., Saburo; R. Eiko; O. Yoshihiko; N. Fumiaki; O. Yoshiharu; S. Hiroyuki; S. Yoshihro. United States, US20050112182, 2005-05-26.

50 F. Hong; Z. Jieyuan; C. Yuquan; L. Xi; W. Jiao. China, CN112794943, 2021-05-14.

51 G. H. Imanzadeh, A. Khalafi-Nezhad, A. Zare, A. Hasaninejad, A. R. Moosavi Zare and A. Parhami, *J. Iran. Chem. Soc.*, 2007, **4**, 229–237.

52 T. P. Nguyen, B. Kim, Y. J. Kim, S. H. Lee, S. Shin and J. K. Cho, *Int J Adhes Adhes*, 2018, **80**, 60–65.

53 S. Mu, Y. Zhang, J. Zhou, B. Wang and Z. Wang, *ACS Sustain Chem Eng*, 2020, **8**, 5296–5304.

54 T. A. Gawargy, B. Wang and J. C. Scaiano, *Photochem Photobiol*, 2022, **98**, 429–433.

55 Q. Xu, J. Lo and S.-W. Lee, *Appl. Sci.*, 2020, **10**, 3384.

56 G. A. Pitsevich, I. Y. Doroshenko, V. E. Pogorelov, L. G. M. Pettersson, V. Sablinskas, V. V. Sapeshko and V. Balevicius, *J Appl Spectrosc*, 2016, **83**, 350–357.

57 L. Ning, W. De-Ning and Y. Sheng-Kangt, *Crystallinity and hydrogen bonding of hard segments in segmented poly(urethane urea) copolymers*, 1996, vol. 37.

58 G. M. Lari, G. Pastore, C. Mondelli and J. Pérez-Ramírez, *Green Chem.,* 2018, **20**, 148–159.

59 C. v. Pramod, R. Fauziah, K. Seshan and J. P. Lange, *Catal Sci Technol*, 2018, **8**, 289–296.

60 J. G. H. Hermens, A. Jensma and B. L. Feringa, *Ang. Chem. Int. Ed.* 2022, **61**, e202112618.